

# REPAIR: REnormalizing Permuted Activations for Interpolation Repair

Keller Jordan<sup>\*1</sup>, Hanie Sedghi<sup>2</sup>, Olga Saukh<sup>3</sup>, Rahim Entezari<sup>3</sup>, and Behnam Neyshabur<sup>2</sup>

<sup>1</sup>Hive AI

<sup>2</sup>Google Research

<sup>3</sup>TU Graz / CSH Vienna

## Abstract

In this paper we look into the conjecture of Entezari *et al.* (2021) which states that if the permutation invariance of neural networks is taken into account, then there is likely no loss barrier to the linear interpolation between SGD solutions. First, we observe that neuron alignment methods alone are insufficient to establish low-barrier linear connectivity between SGD solutions due to a phenomenon we call *variance collapse*: interpolated deep networks suffer a collapse in the variance of their activations, causing poor performance. Next, we propose REPAIR (REnormalizing Permuted Activations for Interpolation Repair) which mitigates variance collapse by rescaling the preactivations of such interpolated networks. We explore the interaction between our method and the choice of normalization layer, network width, and depth, and demonstrate that using REPAIR on top of neuron alignment methods leads to 60%-100% relative barrier reduction across a wide variety of architecture families and tasks. In particular, we report a 74% barrier reduction for ResNet50 on ImageNet and 90% barrier reduction for ResNet18 on CIFAR10. Our code is available at <https://github.com/KellerJordan/REPAIR>.

## 1 Introduction

Training a neural network corresponds to optimizing a highly non-linear function by navigating a complex loss landscape with numerous minima, symmetries and saddles (Zhang *et al.*, 2017; Keskar *et al.*, 2017; Draxler *et al.*, 2018; Şimşek *et al.*, 2021). Overparameterization is one of the reasons behind the abundance of minima leading to different functions that behave similarly on the training data (Neyshabur *et al.*, 2017; Nguyen *et al.*, 2018; Li *et al.*, 2018; Liu *et al.*, 2020). Another reason is the existence of permutation and scaling invariances which lead to functionally identical minima that differ in the weight space (Brea *et al.*, 2019; Entezari *et al.*, 2021). Due to the relationship of the loss landscape with generalization and optimization, a large body of recent works (Li *et al.*, 2017; Mei *et al.*, 2018; Geiger *et al.*, 2019; Nguyen *et al.*, 2018; Fort *et al.*, 2019; Şimşek *et al.*, 2021; Juneja *et al.*, 2022) study the loss landscape of deep neural networks with the goal of navigating the optimizer to a region with desired properties, *e.g.*, with respect to flatness around the SGD solution (Baldassi *et al.*, 2020; Pittorino *et al.*, 2020).

Early work conjectured the existence of a *non-linear* path of non-increasing loss between solutions found by SGD (Freeman and Bruna, 2016; Draxler *et al.*, 2018) and empirically showed how to find it (Garipov *et al.*, 2018; Tatsoy *et al.*, 2020; Pittorino *et al.*, 2022). *Linear* paths between SGD solutions are investigated by Nagarajan and Kolter (2019), who studied MLPs trained from the same initialization on disjoint subsets of MNIST. Frankle *et al.* (2020) studied linear mode connectivity at a larger scale, and focused on different samples of SGD noise rather than disjoint samples of data. Frankle *et al.* (2020) also showed the correspondence between linear mode connectivity and Lottery Ticket Hypothesis (Frankle and Carbin, 2019) *i.e.*, solutions

---

\*This collaboration was facilitated by ML Collective

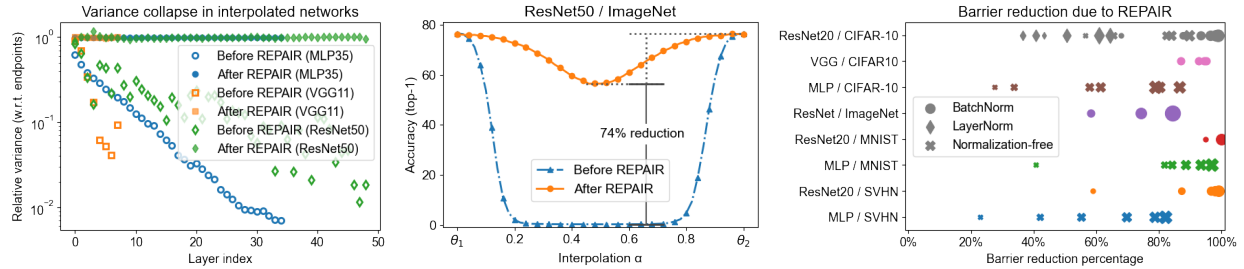


Figure 1: **REPAIR improves the performance of interpolated networks by mitigating variance collapse.** In each experiment, we interpolate between the weights of two independently trained networks whose hidden units have been aligned using the method described in Section 2.3. We then compare the interpolated network before and after applying our correction method REPAIR. **Left:** The variance of activations in interpolated networks progressively collapses. We report the average variance across each layer, normalized by that of the corresponding layer in the original endpoint networks. REPAIR is designed to correct this phenomenon. **Middle:** REPAIR reduces the barrier to linear interpolation between aligned ResNet50s independently trained on ImageNet by 74% (from 76% to 20%). **Right:** REPAIR reduces the interpolation barrier across many choices of architecture, training dataset, and normalization layer. For each architecture/dataset pair we vary the network width; larger markers indicate wider networks.

that are linearly connected with no barrier have the same lottery ticket. Recently, Entezari et al. (2021) conjectured the existence of such a *linear* path between SGD solutions if the permutation invariance of neural networks’ weight space is taken into account. That is, with high probability over SGD solutions, for each pair of trained networks A and B there exists a permutation of the hidden units in each layer of B such that the linear path between A and the permuted network B (B’) is of non-increasing loss relative to the endpoints. This conjecture is important from both theoretical and empirical perspectives. Theoretically, it leads to a drastic simplification of the loss landscape, reducing the complexity obstacle for analyzing deep neural networks. Empirically, linear interpolation between neural network weights has become an important tool, having recently been used to set state of the art accuracy on ImageNet (Wortsman et al., 2022a), improve robustness of finetuned models (Wortsman et al., 2022b; Ilharco et al., 2022), build effective weight-space model ensembles (Izmailov et al., 2019; Frankle et al., 2020; Guo et al., 2022), and constructively merge models trained on separate data splits (Wang et al., 2020; Ainsworth et al., 2022). Therefore, any improvements toward reducing the obstacles to interpolation between trained models has the potential to lead to empirical progress in the above areas.

Prior and concurrent works on linear interpolation (Singh and Jaggi, 2020; Entezari et al., 2021; Ainsworth et al., 2022) have focused on improving the algorithms used to bring the hidden units of two networks into alignment, in order to reduce the barrier to interpolation between them. Singh and Jaggi (2020) develop a strong optimal transport-based method which allows linear interpolation between a pair of ResNet18 (He et al., 2016) networks such that the minimum accuracy attained along the path is 77%. This constitutes a “barrier” of 16% relative to the original endpoint networks which achieve over 93% accuracy on the CIFAR-10 test set. Entezari et al. (2021) use an approach based on simulated annealing (Zhan et al., 2016) in order to find permutations such that wide multi-layer perceptrons (MLPs) (Rosenblatt, 1958) trained on MNIST (LeCun, 1998) can be linearly interpolated with a barrier of nearly zero. Ainsworth et al. (2022) make the first demonstration of zero-barrier connectivity between wide ResNets trained on CIFAR-10 by replacing<sup>1</sup> the standard Batch Normalization (Ioffe and Szegedy, 2015) layers with Layer Normalization (Ba et al., 2016), and develop several novel alignment methods. Further discussion of related work can be found in Appendix A. Given this context, in this paper we are interested in understanding why alignment of the endpoint networks alone has so far been insufficient to reach low-barrier linear connectivity between standard deep convolutional networks.

<sup>1</sup>See the code release, <https://github.com/samuela/git-re-basin/blob/main/src/resnet20.py#L18>

**Contributions** In this work we focus on understanding the source of the poor performance of standard deep networks (ResNet18, VGG11) whose weights have been linearly interpolated from between pairs of networks with aligned neurons. Our contributions are as follows:

- We find that such interpolated networks suffer from a phenomenon of *variance collapse* in which their hidden units have significantly smaller activation variance compared to the corresponding units of the original networks from which they were interpolated. We further identify and explain the reason behind this variance collapse. (Figure 1 (left) and Section 3).
- We propose REPAIR (REnormalizing Permuted Activations for Interpolation Repair), a method that corrects variance collapse by rescaling hidden units in the interpolated network such that their statistics match those of the original networks. (Section 4).
- We demonstrate that applying REPAIR to such interpolated networks leads to significant barrier reductions across a wide variety of architectures, datasets, normalization techniques, and network width/depth (Section 5 and Figure 1 (middle and right)).

## 2 Preliminaries

In this section we give preliminary definitions and algorithms which will be used throughout the paper. In summary, we first present the notion of interpolation between networks, and define the linear interpolation barrier. We then discuss the existence of permutation symmetries in weight space, and present algorithms used to locate such permutations in order to bring the hidden units of two networks into alignment.

### 2.1 Linear interpolation of neural networks

We consider the problem of interpolating between independently trained neural networks. That is, if we let  $\theta_1, \theta_2$  be the weight vectors of two such networks, then we are interested in networks whose weights are of the form  $\theta_\alpha = (1 - \alpha)\theta_1 + \alpha\theta_2$  for  $0 < \alpha < 1$ . We refer to such networks  $\theta_\alpha$  as *interpolated networks*, and to  $\theta_1, \theta_2$  as the *endpoint networks*.

The *loss barrier*  $B(\theta_1, \theta_2)$  between a pair of networks is defined (Entezari et al., 2021) as the maximum increase in loss along the linear path between  $\theta_1$  and  $\theta_2$ , relative to the corresponding convex combination of the two endpoint losses. In notation:

$$B(\theta_1, \theta_2) = \sup_{\alpha \in [0,1]} \left[ \mathcal{L}((1 - \alpha)\theta_1 + \alpha\theta_2) \right] - \left[ (1 - \alpha)\mathcal{L}(\theta_1) + \alpha\mathcal{L}(\theta_2) \right]. \quad (1)$$

The barrier between pairs of unmodified, independent SGD solutions  $\theta_1, \theta_2$  is typically large. We next discuss permutation invariance in neural networks.

### 2.2 Permutation invariance

For typical neural architectures, the neurons in each layer can be permuted without functionally changing the network; this is known as the *permutation invariance* property. In a simple feedforward network, this amounts to the observation that we can replace the  $L$ th weight matrix by  $PW_L$  and the  $(L + 1)$ th weight by  $W_{L+1}P^{-1}$  without changing the function represented by the network. As a result, even if our two networks  $\theta_1, \theta_2$  have learned a functionally identical set of neurons at each layer, it is possible for such neurons to be arbitrarily permuted or misaligned.

Entezari et al. (2021) conjecture that if permutation invariance is taken into account, then all SGD solutions for a sufficiently wide network trained on the same task become linearly mode connected, *i.e.*, have no barrier between them. For completeness we provide the formal statement of the conjecture below.

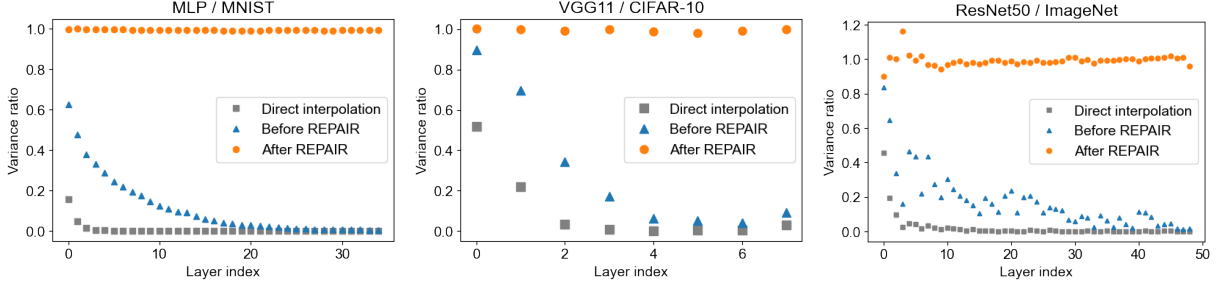


Figure 2: **Variance collapse phenomenon in averaged networks.** We find that the hidden units of weight-space averaged neural networks suffer from *variance collapse*: as we progress through the network, variance of neuron activations reduces, with neurons in deeper layers becoming nearly constant while varying the input data. *Before REPAIR* refers to networks which are interpolated from endpoint networks whose hidden units have been aligned (Li et al., 2015; Singh and Jaggi, 2020; Ainsworth et al., 2022), before our correction method REPAIR is applied. REPAIR is applied on top of this baseline in order to restore the internal statistics of averaged networks back to the level of the endpoint networks.

**Conjecture 1** (Entezari et al., 2021) *For a given neural architecture, let  $\mathcal{P}$  be the set of all valid permutations of hidden units, and  $P : \mathbb{R}^k \times \mathcal{P} \rightarrow \mathbb{R}^k$  be the function that applies a given permutation to a weight vector and returns the permuted version. Then for sufficiently wide networks the following holds: There exists a set of solutions  $\mathcal{S} \subseteq \mathbb{R}^k$  and a function  $Q : \mathcal{S} \rightarrow \mathcal{P}$  such that for any  $\theta_1, \theta_2 \in \mathcal{S}$ , we have small interpolation barrier  $B(P(\theta_1, Q(\theta_1)), \theta_2) \approx 0$  and with high probability over an SGD solution  $\theta$ , we have  $\theta \in \mathcal{S}$ .*

### 2.3 Neuron alignment algorithms

A number of works have proposed methods of finding such alignments between the hidden units of a pair of neural networks. Li et al. (2015) propose to maximize the sum of correlations between the activations of paired neurons across a batch of training data. That is, if we let  $X_{l,i}^{(0)}$  and  $X_{l,i}^{(1)}$  be random variables corresponding to the activations of the  $i$ -th hidden units of the  $l$ -th layer (across a batch of training data), then Li et al. (2015) proposes to optimize the permutation  $P_l$  to maximize the following objective:

$$\sum_i \text{corr}(X_{l,i}^{(1)}, X_{l,P_l(i)}^{(0)}). \quad (2)$$

This amounts to a linear sum assignment problem corresponding to the matrix of correlations between pairs of hidden units in the two networks; which can be solved via the Hungarian algorithm (Kuhn, 1955). Recent works have proposed alternative approaches: He et al. (2018) compute Hessian approximation to align functionally similar neurons, and Singh and Jaggi (2020) develop an optimal transport-based method of soft-alignment. Ainsworth et al. (2022) compare three methods, including one based on that of Li et al. (2015) and two novel approaches.

Tatro et al. (2020) also perform alignment based on minimizing Equation 2, in order to reduce the barrier to non-linear interpolation. Furthermore, they show using a proximal alternating minimization scheme that alignments found using this method are nearly optimal for their purposes. In this paper, we stick with what works and continue to use this alignment method which was originally introduced by Li et al. (2015).

We note that for networks with residual connections, care must be taken to restrict the set of permutations such that the function represented by the network does not change. In particular, the same permutation of hidden units must be applied to all layers which feed into a single residual stream.

### 3 Variance collapse in interpolated networks

In this section we commence our study of interpolated networks. We pick up where previous works left off:

- The barrier between aligned networks decreases with width, including to nearly zero for very wide MLPs trained on MNIST. The barrier also increases sharply with depth, becoming large for MLPs or simple CNNs of more than a few layers (Entezari et al., 2021).
- Even strong optimal transport-based methods, which go far beyond alignment by allowing each neuron in network A to be matched to a weighted sum of neurons in network B, are insufficient to achieve low-barrier (below 5% test-error) connectivity between standard ResNets (Singh and Jaggi, 2020).

We focus on understanding the source of this sharp increase in barrier between aligned networks as a function of depth observed in Entezari et al. (2021), which we hypothesize to be the same phenomenon that causes a high barrier to interpolation for standard ResNets.

#### 3.1 Identifying the problem: Variance Collapse

What causes this rapid drop-off in the performance of interpolated networks which are deeper than a few layers? To answer this question, we investigate the internal behavior of such networks, focusing on the statistics of hidden units (Figure 2). We find that for deep MLPs, interpolated from a pair of aligned endpoint networks which both have high accuracy on the MNIST test-set, hidden units undergo a *variance collapse*. That is, the variance of their activations progressively decays as we move deeper into the network, with the activations of later layers becoming nearly constant. For each layer, we quantify this decay as follows. First, we measure the variance of the activations of each neuron across a batch of training data. We then take the sum of this variance across each neuron in the layer. Finally, if we let this sum be denoted  $v_\alpha, v_1, v_2$  for the interpolated and two endpoint networks, respectively, then we report the ratio  $\frac{v_\alpha}{(v_1+v_2)/2}$ . We compute this ratio for each layer in the network, giving a sequence of values which we report in Figure 2 (left). For the set of variances of each neuron in a single layer of an interpolated ResNet18, see Figure 3 (left).

We observe that variance decays to nearly zero by the final layer of an interpolated 35-layer MLP, indicating that the activations in these last layers have become nearly constant. This effect seems to be further exacerbated when directly interpolating between unaligned networks. We repeat this experiment for VGG (Simonyan and Zisserman, 2014) and ResNet50 architectures, trained on CIFAR-10 and ImageNet respectively, and find that variance by the final layers decays by more than  $10\times$  (Figure 2 (middle) and Figure 2 (right)). This is a problem: if these networks have nearly constant activations in their final layers, then they will no longer even be able to differentiate between inputs.

#### 3.2 Why does this phenomenon occur?

We argue that this phenomenon can be understood through the following statistical calculation. Consider a hidden unit or channel in the first layer of the interpolated network. Such a unit will be functionally equivalent to the linear interpolation between the respective units in the endpoint networks. That is, if we represent the unit’s preactivation by  $X_\alpha$  in the interpolated network, and  $X_1, X_2$  in the two endpoint networks (as random variables over the input data distribution), then the equality  $X_\alpha = (1 - \alpha)X_1 + \alpha X_2$  holds. We will argue that the variance of  $X_\alpha$  is typically reduced as compared to that of  $X_1$  or  $X_2$ .

If the two endpoint networks are perfectly aligned and have learned the same features, then we should have  $\text{corr}(X_1, X_2) = 1$ . But in practice, it is more typical for pairs of aligned units (whose alignment minimizes the cost function given by Equation 2) to have a correlation of  $\text{corr}(X_1, X_2) \approx 0.4$ . When considering the

midpoint interpolated network ( $\alpha = 0.5$ ), the variance of  $X_\alpha$  is given by

$$\begin{aligned} \text{Var}(X_\alpha) &= \text{Var}\left(\frac{X_1 + X_2}{2}\right) \\ &= \frac{\text{Var}(X_1) + \text{Var}(X_2) + 2\text{Cov}(X_1, X_2)}{4} \\ &= \frac{\text{std}^2(X_1) + \text{std}^2(X_2) + 2 \cdot \text{corr}(X_1, X_2) \cdot \text{std}(X_1)\text{std}(X_2)}{4} \\ &= \left(\frac{\text{std}(X_1) + \text{std}(X_2)}{2}\right)^2 - \frac{(1 - \text{corr}(X_1, X_2))}{2} \text{std}(X_1)\text{std}(X_2). \end{aligned}$$

We typically have  $\text{std}(X_1) \approx \text{std}(X_2)$ , so that this simplifies to  $\text{Var}(X_\alpha) = (0.5 + 0.5 \cdot \text{corr}(X_1, X_2)) \cdot \text{Var}(X_1)$ . With our typical value of  $\text{corr}(X_1, X_2) \approx 0.4$  for aligned networks, this yields  $\text{Var}(X_\alpha) = 0.7 \cdot \text{Var}(X_1)$ : a 30% reduction compared to the endpoint networks. This analysis cannot be rigorously extended to deeper layers of the interpolated network, but intuitively we expect this decay to compound with depth. This intuition matches our experiments, where we see that variance collapse becomes worse as we progress through the layers of MLP, VGG, and ResNet50 networks (Figure 2).

## 4 REPAIR

We propose two methods for addressing variance collapse. Both aim to correct the statistics of hidden units in the interpolated network. We call these methods REPAIR (REnormalizing Permutated Activations for Interpolation Repair).

Given an interpolated network  $\theta_\alpha = (1 - \alpha) \cdot \theta_1 + \alpha \cdot \theta_2$  for some  $0 < \alpha < 1$  (with aligned endpoint networks  $\theta_1, \theta_2$ ), we select the set of hidden units or channels whose statistics we aim to correct. For example, for VGG networks we correct the preactivations of every convolutional layer. For ResNets we correct both these convolutional preactivations and the outputs of each residual block.

Our goal will be to compute a set of affine (rescale-and-shift) coefficients for every selected channel, such that the statistics of all selected channels are corrected. Let us consider a particular channel, *e.g.*, the 45th convolutional channel of the 8th layer in an interpolated ResNet18. Similar to the analysis in the last section, let  $X_1$  and  $X_2$  be the values of the channel in the two endpoint networks, viewed as random variables over the input training data, and let  $X_\alpha$  be the same channel in the interpolated network. Then we want the following two conditions to hold:

$$\mathbb{E}[X_\alpha] = (1 - \alpha) \cdot \mathbb{E}[X_1] + \alpha \cdot \mathbb{E}[X_2], \tag{3}$$

$$\text{std}(X_\alpha) = (1 - \alpha) \cdot \text{std}(X_1) + \alpha \cdot \text{std}(X_2). \tag{4}$$

Whereas before any correction, we typically have  $\text{std}(X_\alpha) \ll \min(\text{std}(X_1), \text{std}(X_2))$  due to variance collapse. In the following, we present two algorithms to compute the appropriate sets of affine coefficients for each selected channel, in order to induce these conditions.

Both algorithms depend upon the computation of the statistics  $\mathbb{E}[X_1]$ ,  $\mathbb{E}[X_2]$ ,  $\text{std}(X_1)$ ,  $\text{std}(X_2)$  for each selected channel in the endpoint networks. We present a PyTorch-based approach to perform this computation in Appendix B.2.

### 4.1 Closed-form approximate variant

We first present an efficient, approximate algorithm which computes the desired affine coefficients without using forward-passes in the interpolated network. Consider a hidden unit in the first layer of the interpolated network. As before, let  $X_\alpha$  represent the unit in the interpolated network, and  $X_1, X_2$  the same unit in the two endpoint networks, respectively. Condition (3) will already be satisfied for this unit by virtue of the

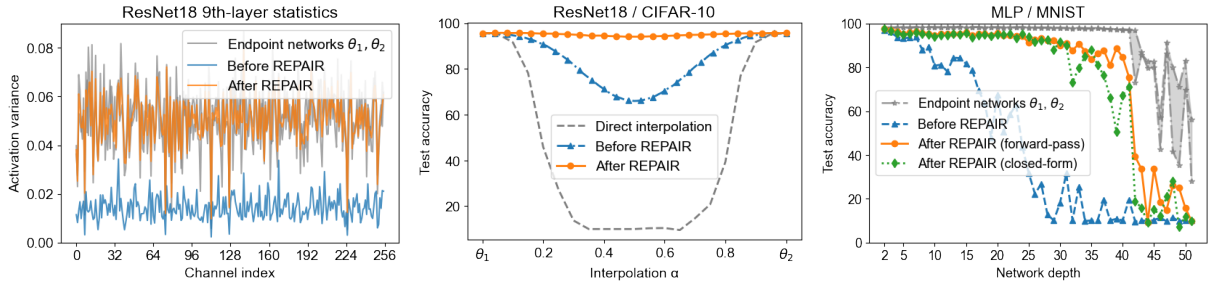


Figure 3: **REPAIR restores the internal statistics of averaged neural networks.** **Left:** We visualize the statistics of different channels in 9th layer of an interpolated ResNet18 on CIFAR-10. The uncorrected network undergoes variance collapse, whereas REPAIR restores the internal statistics of the network to be similar to the endpoint networks. **Middle:** After applying REPAIR, internal statistics are restored, and barrier is reduced to 1.5% for CIFAR-10. **Right:** Permuted interpolation without a statistical correction (before REPAIR) only performs well when limited to MLPs of a few layers (Entezari et al., 2021). REPAIR enables high-performance weight-space averaging between much deeper aligned MLPs.

equation  $X_\alpha = (1 - \alpha) \cdot X_1 + \alpha \cdot X_2$ . Given the values  $\text{Var}(X_1)$ ,  $\text{Var}(X_2)$ , and  $\text{Cov}(X_1, X_2)$ , it is possible to compute the variance of  $X_\alpha$  exactly according to the formula

$$\text{Var}(X_\alpha) = (1 - \alpha)^2 \text{Var}(X_1) + \alpha^2 \text{Var}(X_2) + 2\alpha(1 - \alpha) \text{Cov}(X_1, X_2). \quad (5)$$

Therefore, to satisfy condition (4) for this unit, the rescaling coefficient  $\beta$  must be

$$\beta = \frac{(1 - \alpha) \cdot \text{std}(X_1) + \alpha \cdot \text{std}(X_2)}{\sqrt{(1 - \alpha)^2 \text{Var}(X_1) + \alpha^2 \text{Var}(X_2) + 2\alpha(1 - \alpha) \text{Cov}(X_1, X_2)}},$$

which is simply the desired standard deviation divided by the standard deviation of  $X_\alpha$ . For each unit in the first layer, this factor is exactly correct in order to obtain the desired statistics. For deeper layers, this factor is an approximation which we empirically test.

In Figure 3 (right), we apply this rescaling to every hidden unit of MLPs of depth between 2 and 50 hidden layers, which are linearly interpolated ( $\alpha = 0.5$ ) between aligned endpoints networks trained on MNIST. We find that this rescaling significantly improves the performance of such interpolated networks. In particular, we obtain interpolated checkpoints of up to 27 layers that achieve over 90% accuracy, whereas without a correction, we hit this limit after only 6 layers.

We note that this correction requires forward passes in the endpoint networks in order to compute the values of  $\text{Var}(X_1)$ ,  $\text{Var}(X_2)$ , and  $\text{Cov}(X_1, X_2)$  for each hidden unit. Once these values have been computed, correction coefficients to interpolated networks across arbitrary choice of interpolation coefficient  $\alpha$  can be generated without requiring any further forward passes.

## 4.2 Forward-pass exact variant

The rescaling coefficients generated by the above algorithm are approximate, only being guaranteed to induce the desired conditions (3), (4) for hidden units or channels in the first layer of an interpolated network. We find that it is effective for the case of deep MLPs, but in our experiments it was insufficient to significantly reduce the interpolation barrier for more challenging cases like ResNet50 trained on ImageNet. We now propose an exact algorithm, which uses forward passes in the interpolated networks in order to generate affine (rescale-and-shift) parameters for every channel in the network that we aim to correct. This method outperforms the approximate variant, especially for challenging cases.

The exact method proceeds as follows. For each module in the interpolated network whose outputs we have identified as targets for statistical correction, we apply a wrapper, PyTorch pseudocode for which

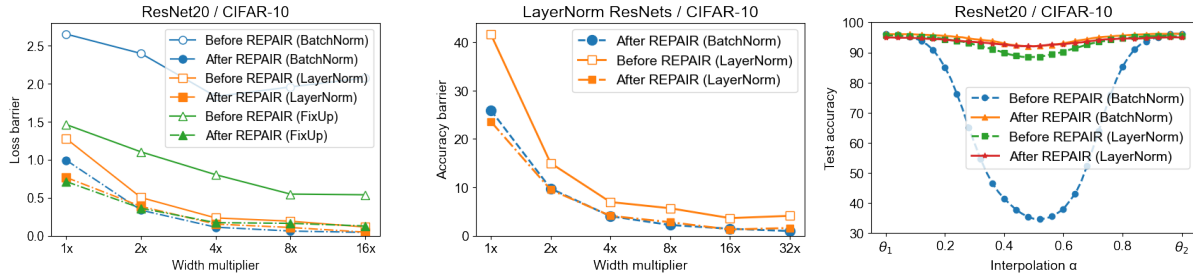


Figure 4: **Effect of normalization layer.** **Left:** Loss barriers with and without REPAIR for ResNet20s trained with BatchNorm, LayerNorm, and normalization-free via FixUp, varying the width multiplier from 1 to 16. **Middle:** LayerNorm networks are unique in reaching a relatively low barrier before REPAIR. **Right:** Performance curves of networks interpolated between aligned ResNet20s. Without REPAIR, the midpoint BatchNorm-based network achieves 34.7% accuracy, compared to 88.4% for LayerNorm. After REPAIR, both variants attain 92.0% accuracy.

can be found in Appendix B.2. This wrapper adds a Batch Normalization layer after the wrapped module which is initially set to “train” mode. Each such added BatchNorm layer contains affine (*i.e.*, per-channel rescale-and-shift) parameters. For a given channel incoming to the BatchNorm layer, we set the respective affine weight to  $(1 - \alpha) \text{std}(X_1) + \alpha \text{std}(X_2)$  and the bias to  $(1 - \alpha) \mathbb{E}[X_1] + \alpha \mathbb{E}[X_2]$ , where  $X_1$  and  $X_2$  are the respective channels in the endpoint networks as in conditions (3), (4).

With the added BatchNorm layers in training mode, these affine parameters will exactly induce our statistical conditions with respect to batches of input data. The reason for this is that during execution, the added BatchNorm layers first renormalize their inputs to have zero mean and unit variance per channel, and then apply our given affine transformation which sets the statistics of the output to be that of conditions (3), (4). Next, we pass a set of training data through the network ( $\sim 5,000$  examples suffices) so that the running mean and variance parameters of our added BatchNorm layers will be accurately estimated. During this pass, any BatchNorm layers which already existed in the original network are kept frozen. Finally, we set the added BatchNorm layers to evaluation mode, so that they behave as affine layers which do not recompute statistics. At this point, the resulting network is functionally equivalent to one in which the weights of our selected set of channels have been rescaled and biases shifted. If we wish to generate a new parameter vector  $\theta'_\alpha$  which is compatible with the original network architecture (*i.e.*, lacks these added BatchNorm layers), then we can perform BatchNorm layer fusion (Markuš, 2018) in which appropriate rescaling and bias-shifting values are computed from each added BatchNorm layer, and then applied to the preceding convolutional filters.

The networks resulting from this process have their internal statistics corrected, so that all selected channels satisfy conditions (3), (4). In Figure 3 (left) we observe that REPAIR has resolved variance collapse. In Figure 3 (middle) we apply REPAIR to networks where the weights are linearly interpolated between a pair of ResNet18s whose hidden units have been brought into alignment. Before the correction, networks near the midpoint have a reduced accuracy of 66.0% on the CIFAR-10 test set, while the endpoints accuracy is 95.5%. After correction, all checkpoints along the linear path have significantly boosted accuracy, with the midpoint performing at 94.1%. In comparison, Singh and Jaggi (2020) report a linear midpoint accuracy of 77.0% using strong optimal-transport based alignment methods to improve over the baseline.

Throughout the rest of the paper, we refer to the above method as REPAIR. We note that the utility of this method is orthogonal to any improvements in the algorithm used to align the hidden units of the endpoint networks. We explore this in Appendix Figure 14, where we report barrier curves for REPAIR applied to interpolations between unaligned networks as well. In the remainder of the paper, we demonstrate the effectiveness of REPAIR across a wide range of scenarios.



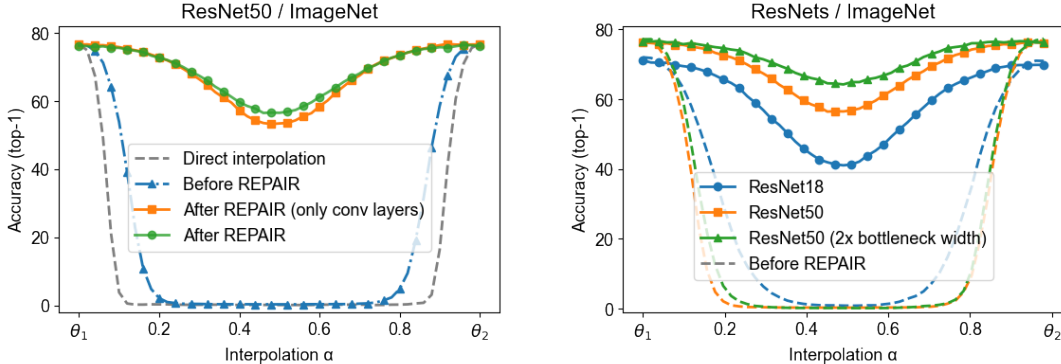


Figure 5: **REPAIR significantly reduces barrier between ResNet50s trained on ImageNet.** **Left:** Without REPAIR, interpolations between two aligned, independently trained ResNet50s attain less than 1% test accuracy on ImageNet. After applying REPAIR to convolutional layer outputs, the midpoint is boosted to 53.2%. Using full REPAIR, which is also applied to the outputs of residual blocks, this is further boosted to 56.5%. **Right:** Larger and wider ResNet architectures have smaller barrier. Dashed lines indicate the baseline of interpolation between aligned networks (Singh and Jaggi, 2020; Ainsworth et al., 2022), and solid lines refer to REPAIR on top of baseline.

## 5 Experimental results

In this section we report the results of the following experiments.

- We investigate the effectiveness of REPAIR for three variants of ResNet trained on CIFAR-10: standard BatchNorm-based ResNets, nonstandard LayerNorm-based ResNets, and normalization-free ResNets using FixUp (Zhang et al., 2019). (Section 5.1)
- We apply REPAIR to (interpolations between aligned) ResNets trained on ImageNet. (Section 5.2)
- We study the relationship between width and barrier size, with experiments conducted using 10-layer MLPs and standard ResNet20s across four datasets: MNIST, SVHN, FashionMNIST, and CIFAR-10. We also report barriers for VGG networks of varying depth trained on CIFAR-10. (Section 5.3)
- Finally, we perform a replication using REPAIR of an experiment from Ainsworth et al. (2022), in which a pair of models trained on disjoint subsets of data is constructively merged. (Section 5.4)

Extra figures which replicate these experiments in terms of alternate metrics can be found in Appendix C.

### 5.1 Normalization layer

We begin by considering ResNet20s trained on CIFAR-10 using three different types of normalization layer: BatchNorm (Ioffe and Szegedy, 2015), LayerNorm (Ba et al., 2016), and normalization-free via Fixup (Zhang et al., 2019). We combine this ablation with a study on the effect of width: for each class of networks, we vary the width multiplier from  $1\times$ , where the final block has 64 channels, up to  $16\times$  or 1024 channels. In Figure 4 we report the barriers to interpolation, both with and without REPAIR. We find that REPAIR is effective for all three cases, shrinking the loss barrier to below 0.05 for BatchNorm and LayerNorm-based networks when width is scaled to  $16\times$ .

The LayerNorm-based ResNets are a special case that deserves comment. We first note that LayerNorm is nonstandard in ResNets, and has worse performance when compared to BatchNorm; with our training configuration, LayerNorm-based ResNet20s achieve 92.4% CIFAR-10 test set accuracy, vs. 93.6% for the BatchNorm baseline. But these networks also have a unique property: when interpolating between aligned LayerNorm-ResNets, the midpoints already perform relatively well before REPAIR is applied. In Figure 4,

we observe that the midpoint between our pair of  $8\times$ -width LayerNorm-ResNet20s attains 90.3% test-set accuracy, which is boosted to 93.2% by an application of REPAIR. In contrast, for the same width using BatchNorm, the interpolated network obtains only 32.3% accuracy, which is boosted to 94.4% by REPAIR.

One possible explanation for this phenomenon is that LayerNorm can partially mitigate variance collapse because it applies test-time normalization, which may prevent per-layer reductions in variance from compounding through the forward pass. In contrast, BatchNorm is functionally just an affine layer during test-time, so that variance reductions do compound.

We claim that this observation regarding LayerNorm-based ResNets explains the contradiction between the results of [Singh and Jaggi \(2020\)](#) and [Ainsworth et al. \(2022\)](#). In the former, the authors develop a strong optimal-transport based method of aligning networks, which contains the approach of [Li et al. \(2015\)](#) as a special case. They show that even this method is insufficient to attain low-barrier connectivity between standard ResNets before fine-tuning; their best result is a barrier of 16% error between aligned ResNet18s trained on CIFAR-10. In contrast, [Ainsworth et al. \(2022\)](#) report that a variety of alignment methods, including the method of [Li et al. \(2015\)](#) which they call “activation matching”, suffice to establish nearly zero-barrier connectivity between wide ResNets trained on CIFAR-10. How can both results be true? We claim that this contradiction is resolved by the observation that [Ainsworth et al. \(2022\)](#) replace standard BatchNorm layers with LayerNorm in their ResNets, as is evident in the code release<sup>2</sup>. In our experiments, the use of LayerNorm uniquely allows for low-barrier linear connectivity without the requirement of a statistical correction such as REPAIR, at the cost of reduced performance on most datasets.

## 5.2 ImageNet

Next, we explore the impact of REPAIR on the barriers to interpolation between standard ResNet models trained from scratch on ImageNet ([Deng et al., 2009](#)). We test ResNet18, ResNet50, and a double-width variant of ResNet50 in Figure 5 (right). Without REPAIR, the interpolated midpoints between each aligned pair of networks perform at below 1% accuracy on the ImageNet validation set. After REPAIR, the midpoint ResNet18 improves to 41.1%, ResNet50 to 56.5%, and double-width ResNet50 to 64.2%.

We find in Figure 5 (left) that it is important to apply REPAIR not just to all convolutional layer outputs, but also to the outputs of every residual block. For the case of ResNet50, using REPAIR with these extra channels boosted the performance of the midpoint from 53.2% to 56.5%, which is a 14% reduction in the size of the barrier (from 23.4% to 20.1%). We note that for architectures which contain BatchNorm after every convolutional layer, applying REPAIR only to convolutional layer outputs is mathematically equivalent to resetting the BatchNorm statistics of the network. Performing such a reset on averaged networks goes back to ([Izmailov et al., 2018](#)), but as far as we are aware, has not been applied to interpolation between independently trained networks until now. We provide a comparison between the ImageNet results of our work and those of [Ainsworth et al. \(2022\)](#) in Appendix Figure 8.

In general, the barriers for these architectures on ImageNet are still relatively high. The standard ResNet50 architecture has a final-block bottleneck width of 1024, and we measure the barrier after REPAIR to be 20.1% in terms of test error. The double-width ResNet50 variant has a final-block bottleneck width of 2048, reducing the barrier to 12.9%. In comparison, the widest ResNet20 we studied on CIFAR-10 had final-layer width of 1024, and a barrier of nearly zero. Therefore, it may be the case that for more difficult datasets, larger widths are required in order to reach low barriers.

## 5.3 Network width and depth

In Figure 6 (left and middle), we study the impact of our statistical correction across four datasets (MNIST, FashionMNIST ([Xiao et al., 2017](#)), SVHN ([Netzer et al., 2011](#)), and CIFAR-10) and two architectures (10-layer MLP and standard ResNet20). We report the barriers to interpolation in terms of accuracy both before and after REPAIR, varying the width of each network. In all cases, REPAIR is effective in reducing the barrier,

<sup>2</sup><https://github.com/samuella/git-re-basin/blob/main/src/resnet20.py#L18>

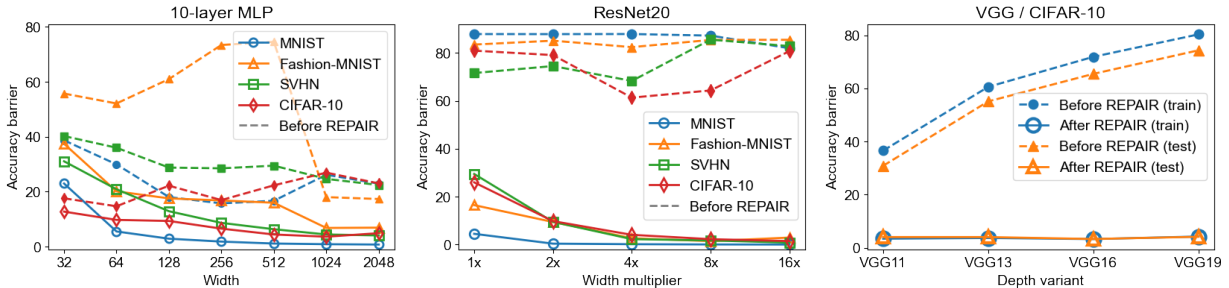


Figure 6: **Network width and depth.** **Left:** We investigate the effect of REPAIR on the barrier for 10-layer MLPs, trained on MNIST, FashionMNIST, SVHN, and CIFAR-10. In each case, the baseline (interpolation between aligned networks) is shown with dotted curve, and the solid curve refers to cases where REPAIR is applied on top of the baseline. We vary the width from 32 to 2048 hidden units per layer. **Middle:** We conduct the same experiment using ResNet20s trained on the same four datasets. We vary the width multiplier from 1 to 16, producing models whose final block ranges from 64 to 1024 channels. **Right:** We investigate the effect of REPAIR on the barrier for VGG networks trained on CIFAR-10. We vary the network depth from 11 to 19 layers, and observe that without REPAIR the barrier increases with depth, whereas with REPAIR it is close to constant in depth.

and the size of the barrier decreases as network width is increased. For MNIST, which is the easiest task, even networks of smaller width are able to reach nearly zero barrier to interpolation.

We also study the effect of network depth, across standard VGG networks of depth varying from 11 to 19 layers. We report the barriers to interpolation between such aligned networks, before and after REPAIR, in Figure 6 (right). Consistently with our earlier results on MLPs, we find that the barrier increases with depth before REPAIR is applied, and afterwards the barrier is small and roughly flat with depth.

## 5.4 Split data training

In this section we study the setting where two endpoint networks are trained on disjoint splits of the training dataset. We aim to replicate the corresponding experiment of Ainsworth et al. (2022), but using REPAIR applied to standard BatchNorm networks.

The experiment proceeds as follows. We first split the CIFAR-100 training set, consisting of 50,000 images distributed across 100 classes, into two disjoint sets of 25,000 images. The first split consists of a random 80% of the images in the first 50 classes, and 20% of the images in the second 50 classes, with the second split having the proportions reversed. We then train two networks, one for each split. The result is that one network is more accurate on the first 50 classes, and the other more accurate on the second, with both performing worse than either their ensemble or a network trained on the full training set.

We next align the hidden units of these two networks, and generate a series of linearly interpolated networks between the two, applying REPAIR to each (Figure 7).

We find that many of these interpolated networks significantly outperform either of the two endpoints in terms of loss on the full CIFAR-100 test set. In this sense, the endpoint networks can be said to have been constructively merged. The best interpolated network of Ainsworth et al. (2022) was reported to obtain a loss of 1.73 at  $\alpha \approx 0.3$ . Using REPAIR, our best interpolated network achieves a test loss of 1.30, also

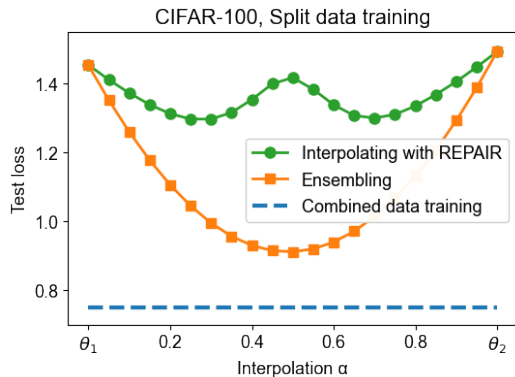


Figure 7: **Split data training.** When two networks are trained on disjoint, biased subsets of CIFAR-100, their REPAIred interpolations outperform either endpoint with respect to the combined test set.

with mixing coefficient  $\alpha = 0.3$ . We attribute this improvement partially to REPAIR, and partially to the increased performance of standard ResNets compared to the LayerNorm-based variants used in [Ainsworth et al. \(2022\)](#). In Appendix C, we compare these results against a strong baseline.

## 6 Discussion and future work

In this paper we proposed REPAIR, a method of mitigating the *variance collapse* phenomenon which we show occurs in interpolated networks. We demonstrated that REPAIR significantly improves the performance of interpolated networks across a wide variety of architectures and datasets. For example, we used REPAIR to reduce the barrier to permuted interpolation for a standard ResNet18 trained on CIFAR-10 from 16% ([Singh and Jaggi, 2020](#)) to 1.5%. Further, we use REPAIR to improve the performance of interpolated ResNet50s from below 1% to 56.5% on ImageNet. REPAIR is effective for networks trained without normalization layers, or with LayerNorm instead of BatchNorm.

To explain these results, we provided an analysis of the variance collapse phenomenon and how REPAIR mitigates it. We also demonstrated that LayerNorm-based networks are unique in attaining a relatively low barrier to aligned interpolation before the use of REPAIR, resolving the contradiction between the results of [Singh and Jaggi \(2020\)](#) and [Ainsworth et al. \(2022\)](#).

In so far as we establish low-barrier permuted interpolation for further scenarios, these results provide support for the conjecture of [Entezari et al. \(2021\)](#). On the other hand, to practically do so we needed to rescale the preactivations of the interpolated network, moving us out of the realm of strictly permuted linear interpolation. Our rescaling REPAIR evolved as a generalization of the method of resetting BatchNorm statistics of averaged networks ([Izmailov et al., 2018](#)). Such a correction appears to be necessary in order to establish low-barrier permuted linear connectivity, at practical widths and without the use of LayerNorm.

On the empirical side, we demonstrated that REPAIred interpolations between two networks which were trained on disjoint, biased dataset splits are able to outperform either network from which they were interpolated. We hope that further such applied results will be possible, including improvements to weight-space ensembling, checkpoint averaging and robust finetuning.

## Acknowledgements

We thank Luke Johnston for his insightful comments on the manuscript.

## References

- Agueh, M. and Carlier, G. (2011). Barycenters in the wasserstein space. *SIAM Journal on Mathematical Analysis*, 43(2):904–924.
- Ainsworth, S. K., Hayase, J., and Srinivasa, S. (2022). Git re-basin: Merging models modulo permutation symmetries. *arXiv preprint arXiv:2209.04836*.
- Ashmore, S. and Gashler, M. (2015). A method for finding similarity between multi-layer perceptrons by forward bipartite alignment. In *2015 International Joint Conference on Neural Networks (IJCNN)*, pages 1–7. IEEE.
- Ba, J. L., Kiros, J. R., and Hinton, G. E. (2016). Layer normalization. *arXiv preprint arXiv:1607.06450*.
- Baldassi, C., Pittorino, F., and Zecchina, R. (2020). Shaping the learning landscape in neural networks around wide flat minima. *Proceedings of the National Academy of Sciences*, 117(1):161–170.
- Brea, J., Simsek, B., Illing, B., and Gerstner, W. (2019). Weight-space symmetry in deep networks gives rise to permutation saddles, connected by equal-loss valleys across the loss landscape. *arXiv preprint arXiv:1907.02911*.

- Deng, J., Dong, W., Socher, R., Li, L.-J., Li, K., and Fei-Fei, L. (2009). Imagenet: A large-scale hierarchical image database. In *2009 IEEE conference on computer vision and pattern recognition*, pages 248–255. IEEE.
- Draxler, F., Veschgini, K., Salmhofer, M., and Hamprecht, F. (2018). Essentially no barriers in neural network energy landscape. In *International conference on machine learning*, pages 1309–1318. PMLR.
- Entezari, R., Sedghi, H., Saukh, O., and Neyshabur, B. (2021). The role of permutation invariance in linear mode connectivity of neural networks. *arXiv preprint arXiv:2110.06296*.
- Fort, S., Hu, H., and Lakshminarayanan, B. (2019). Deep ensembles: A loss landscape perspective. *arXiv preprint arXiv:1912.02757*.
- Frankle, J. and Carbin, M. (2019). The lottery ticket hypothesis: Finding sparse, trainable neural networks.
- Frankle, J., Dziugaite, G. K., Roy, D., and Carbin, M. (2020). Linear mode connectivity and the lottery ticket hypothesis. In *International Conference on Machine Learning*, pages 3259–3269. PMLR.
- Freeman, C. D. and Bruna, J. (2016). Topology and geometry of half-rectified network optimization. *arXiv preprint arXiv:1611.01540*.
- Garipov, T., Izmailov, P., Podoprikin, D., Vetrov, D. P., and Wilson, A. G. (2018). Loss surfaces, mode connectivity, and fast ensembling of dnns. *Advances in neural information processing systems*, 31.
- Geiger, M., Spigler, S., d’Ascoli, S., Sagun, L., Baity-Jesi, M., Biroli, G., and Wyart, M. (2019). Jamming transition as a paradigm to understand the loss landscape of deep neural networks. *Physical Review E*, 100(1):012115.
- Guo, H., Jin, J., and Liu, B. (2022). Stochastic weight averaging revisited.
- He, K., Zhang, X., Ren, S., and Sun, J. (2016). Deep residual learning for image recognition. In *Proceedings of the IEEE conference on computer vision and pattern recognition*, pages 770–778.
- He, X., Zhou, Z., and Thiele, L. (2018). Multi-task zipping via layer-wise neuron sharing. *arXiv preprint arXiv:1805.09791*.
- Hotelling, H. (1992). Relations between two sets of variates. In *Breakthroughs in statistics*, pages 162–190. Springer.
- Ilharco, G., Wortsman, M., Gadre, S. Y., Song, S., Hajishirzi, H., Kornblith, S., Farhadi, A., and Schmidt, L. (2022). Patching open-vocabulary models by interpolating weights. *arXiv preprint arXiv:2208.05592*.
- Ioffe, S. and Szegedy, C. (2015). Batch normalization: Accelerating deep network training by reducing internal covariate shift. In *International conference on machine learning*, pages 448–456. PMLR.
- Izmailov, P., Podoprikin, D., Garipov, T., Vetrov, D., and Wilson, A. G. (2018). Averaging weights leads to wider optima and better generalization. *arXiv preprint arXiv:1803.05407*.
- Izmailov, P., Podoprikin, D., Garipov, T., Vetrov, D., and Wilson, A. G. (2019). Averaging weights leads to wider optima and better generalization.
- Juneja, J., Bansal, R., Cho, K., Sedoc, J., and Saphra, N. (2022). Linear connectivity reveals generalization strategies. *arXiv preprint arXiv:2205.12411*.
- Keskar, N. S., Mudigere, D., Nocedal, J., Smelyanskiy, M., and Tang, P. T. P. (2017). On large-batch training for deep learning: Generalization gap and sharp minima.
- Kuhn, H. W. (1955). The hungarian method for the assignment problem. *Naval Research Logistics (NRL)*, 52.

- LeCun, Y. (1998). The mnist database of handwritten digits. [http://yann. lecun. com/exdb/mnist/](http://yann.lecun.com/exdb/mnist/).
- Li, D., Ding, T., and Sun, R. (2018). Over-parameterized deep neural networks have no strict local minima for any continuous activations. *arXiv preprint arXiv:1812.11039*.
- Li, H., Xu, Z., Taylor, G., Studer, C., and Goldstein, T. (2017). Visualizing the loss landscape of neural nets. *arXiv preprint arXiv:1712.09913*.
- Li, Y., Yosinski, J., Clune, J., Lipson, H., and Hopcroft, J. (2015). Convergent learning: Do different neural networks learn the same representations? *arXiv preprint arXiv:1511.07543*.
- Liu, C., Zhu, L., and Belkin, M. (2020). Loss landscapes and optimization in over-parameterized non-linear systems and neural networks. *arXiv preprint arXiv:2003.00307*.
- Markuš, N. (2018). Fusing batch normalization and convolution in runtime. <https://nenadmarkus.com/p/fusing-batchnorm-and-conv/>. Accessed: 2022-09-28.
- Mei, S., Montanari, A., and Nguyen, P.-M. (2018). A mean field view of the landscape of two-layer neural networks. *Proceedings of the National Academy of Sciences*, 115(33):E7665–E7671.
- Nagarajan, V. and Kolter, J. Z. (2019). Uniform convergence may be unable to explain generalization in deep learning. *Advances in Neural Information Processing Systems*, 32.
- Netzer, Y., Wang, T., Coates, A., Bissacco, A., Wu, B., and Ng, A. Y. (2011). Reading digits in natural images with unsupervised feature learning.
- Neyshabur, B., Bhojanapalli, S., McAllester, D., and Srebro, N. (2017). Exploring generalization in deep learning. In *Proceedings of the 31st International Conference on Neural Information Processing Systems, NIPS’17*, page 5949–5958.
- Nguyen, Q., Mukkamala, M. C., and Hein, M. (2018). On the loss landscape of a class of deep neural networks with no bad local valleys. *arXiv preprint arXiv:1809.10749*.
- Pittorino, F., Ferraro, A., Perugini, G., Feinauer, C., Baldassi, C., and Zecchina, R. (2022). Deep networks on toroids: Removing symmetries reveals the structure of flat regions in the landscape geometry. *arXiv preprint arXiv:2202.03038*.
- Pittorino, F., Lucibello, C., Feinauer, C., Malatesta, E. M., Perugini, G., Baldassi, C., Negri, M., Demyanenko, E., and Zecchina, R. (2020). Entropic gradient descent algorithms and wide flat minima. *arXiv preprint arXiv:2006.07897*.
- Rosenblatt, F. (1958). The perceptron: a probabilistic model for information storage and organization in the brain. *Psychological review*, 65(6):386.
- Simonyan, K. and Zisserman, A. (2014). Very deep convolutional networks for large-scale image recognition. *arXiv preprint arXiv:1409.1556*.
- Şimşek, B., Ged, F., Jacot, A., Spadaro, F., Hongler, C., Gerstner, W., and Brea, J. (2021). Geometry of the loss landscape in overparameterized neural networks: Symmetries and invariances. *arXiv preprint arXiv:2105.12221*.
- Singh, S. P. and Jaggi, M. (2020). Model fusion via optimal transport. *Advances in Neural Information Processing Systems*, 33:22045–22055.
- Tatro, N. J., Chen, P.-Y., Das, P., Melnyk, I., Sattigeri, P., and Lai, R. (2020). Optimizing mode connectivity via neuron alignment. *arXiv preprint arXiv:2009.02439*.

- Uriot, T. and Izzo, D. (2020). Safe crossover of neural networks through neuron alignment. In *Proceedings of the 2020 Genetic and Evolutionary Computation Conference*, pages 435–443.
- Wang, H., Yurochkin, M., Sun, Y., Papailiopoulos, D., and Khazaeni, Y. (2020). Federated learning with matched averaging. *arXiv preprint arXiv:2002.06440*.
- Wortsman, M., Ilharco, G., Gadre, S. Y., Roelofs, R., Gontijo-Lopes, R., Morcos, A. S., Namkoong, H., Farhadi, A., Carmon, Y., Kornblith, S., et al. (2022a). Model soups: averaging weights of multiple fine-tuned models improves accuracy without increasing inference time. In *International Conference on Machine Learning*, pages 23965–23998. PMLR.
- Wortsman, M., Ilharco, G., Kim, J. W., Li, M., Kornblith, S., Roelofs, R., Lopes, R. G., Hajishirzi, H., Farhadi, A., Namkoong, H., et al. (2022b). Robust fine-tuning of zero-shot models. In *Proceedings of the IEEE/CVF Conference on Computer Vision and Pattern Recognition*, pages 7959–7971.
- Xiao, H., Rasul, K., and Vollgraf, R. (2017). Fashion-mnist: a novel image dataset for benchmarking machine learning algorithms. *arXiv preprint arXiv:1708.07747*.
- Zhan, S.-h., Lin, J., Zhang, Z.-j., and Zhong, Y.-w. (2016). List-based simulated annealing algorithm for traveling salesman problem. *Intell. Neuroscience*, 2016:8.
- Zhang, C., Bengio, S., Hardt, M., Recht, B., and Vinyals, O. (2017). Understanding deep learning requires rethinking generalization. In *Proceedings of the International Conference on Learning Representations*.
- Zhang, H., Dauphin, Y. N., and Ma, T. (2019). Fixup initialization: Residual learning without normalization. *arXiv preprint arXiv:1901.09321*.

# Appendix

## A Further discussion of related work

Entezari et al. (2021) try to find a low-barrier permutation between two SGD solutions by searching in the set of all permutations using simulated annealing. Neuron alignment methods use efficient heuristics to find a matching that maximizes a defined similarity measure given two neural networks (Li et al., 2015; Ashmore and Gashler, 2015; Singh and Jaggi, 2020; Tatrot et al., 2020; Pittorino et al., 2022). This similarity measure is often based on correlation between weights or activations of the neurons in the same layer. Prior work was unable to achieve low-barrier for many standard architectures and/or challenging tasks (*e.g.*, ImageNet classification).

Uriot and Izzo (2020) use the neuron representation introduced in Li et al. (2015) to perform alignment between different feedforward networks (which they refer to as a crossover between parents). They consider two ways of characterizing the relationships between neurons: Canonical Correlation Analysis (Hotelling, 1992)<sup>3</sup> and pairwise cross-correlation (Li et al., 2015), and apply alignment operators depending on the uncovered relationship. He et al. (2018) propose a neuron alignment method in the context of multi-task model compression. The algorithm leverages layer-wise Hessian approximation to match neurons by computing a similarity measure based on their functional difference. Singh and Jaggi (2020) propose a model fusion algorithm which leverages optimal transport to perform neuron alignment in the Wasserstein space (Agueh and Carlier, 2011), achieving a barrier of 16% for ResNet18 trained on CIFAR-10; furthermore they show that by finetuning such interpolated networks, the original performance is recovered.

Tatrot et al. (2020) point out that special care must be taken for networks that contain batch normalization layers when it comes to neuron alignment. They match neurons by optimizing a curve in the weight space between two models by aligning correlations of post-activations. The running statistics are normalized by training the model for one epoch, while freezing all learnable parameters of the model. However, the crucial role of statistics reset in the context of linear interpolation of the models is not investigated. A recent work by Pittorino et al. (2022) uses LayerNorm as part of symmetry removal, so that the network behavior remains unchanged.

## B Implementation details

### B.1 Training hyperparameters

Table 1 summarizes the hyperparameters we used to train the neural networks which appear in this work.

- We train all networks using SGD with momentum 0.9. The weight decay and learning rates differ for each task, and are specified below.
- For our MLP trainings, we keep the hyperparameters below constant across varying widths, depths, and datasets.
- When training on MNIST and SVHN, we remove cutout and horizontal flip from the list of data augmentations used by our ResNet20 training. Otherwise, we keep the below ResNet20 hyperparameters constant across different choices of width, dataset, and normalization layer.

### B.2 PyTorch wrapper module pseudocode

1. The first step of REPAIR is to measure the statistics of identified channels in the endpoint networks. There are many ways to do this, but we found that the following was efficient and had low code-

---

<sup>3</sup>Canonical Correlation Analysis is a multivariate statistical technique that finds maximally correlated linear relationships between two sets of observations, under orthogonality and norm constraints.



Table 1: Training hyperparameters

Hyper-parameters	MLP	VGG	ResNet20	ResNet50/ImageNet
Batch Size	2000	500	500	512
Epochs	100	100	200	300
Learning Rate	Linear 0.2	Cosine 0.08	Cosine 0.4	Linear 0.5
Weight decay	0.0	0.0005	0.0001	0.0001
Data augmentation	Translate	Flip+Translate	Flip+Translate+Cutout	Flip+RandomResizedCrop

complexity in a Pytorch environment. For each module in the interpolated network whose outputs we wish to REPAIR, we wrap the corresponding modules in the endpoint networks with the following:

---

```

class TrackLayer(nn.Module):
    def __init__(self, layer):
        super().__init__()
        self.layer = layer
        self.bn = nn.BatchNorm2d(len(layer.weight))
        self.bn.train()
        self.layer.eval()
    def get_stats(self):
        return (self.bn.running_mean, self.bn.running_var.sqrt())
    def forward(self, inputs):
        outputs = self.layer(inputs)
        # Apply BatchNorm so that the running mean/variance are updated; discard the output.
        self.bn(outputs)
        return outputs

```

---

It then suffices to pass a small set of training data (~5,000 examples) through the tracked endpoint networks. At this point, the statistics of each tracked module’s output can be retrieved from the wrapping TrackLayer.

- Next, we wrap each module in the interpolated network that we wish to REPAIR with the following:

---

```

class ResetLayer(nn.Module):
    def __init__(self, layer):
        super().__init__()
        self.layer = layer
        self.bn = nn.BatchNorm2d(len(layer.weight))
    def set_stats(self, goal_mean, goal_std):
        self.bn.bias.data = goal_mean
        self.bn.weight.data = goal_std
    def forward(self, x):
        return self.bn(self.layer(x))

```

---

The next step is to iterate over each triple of corresponding (TrackLayer, TrackLayer, ResetLayer) modules coming from the two endpoint networks and the interpolated network. For each triple, we set the statistics of the ResetLayer to be the interpolation of the statistics from the two TrackLayers. Working and minimal code to accomplish this can be found in our code release.

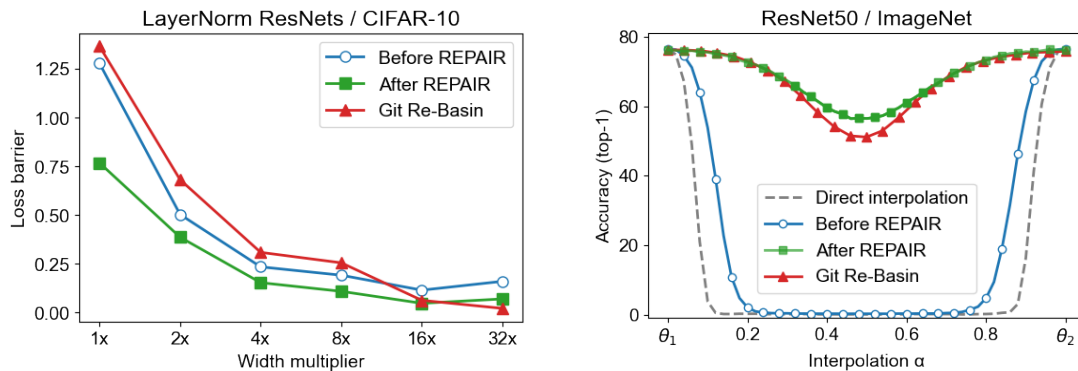


Figure 8: **Comparison to Ainsworth et al. (2022).** **Left:** We compare barrier values of LayerNorm-based ResNets, for our baseline and REPAIR, to the barriers reported in Ainsworth et al. (2022). We find that for networks of width up to  $8\times$ , our baseline barrier values are comparable, indicating that our baseline alignment method (Li et al., 2015) performs similarly to those explored in Ainsworth et al. (2022). With REPAIR, our barrier values are lower. For the case of  $32\times$ -width networks, our barrier value is higher than that reported in Ainsworth et al. (2022). **Right:** We compare our results on ImageNet using REPAIR with those of Ainsworth et al. (2022). We note that in their ImageNet experiments, Ainsworth et al. (2022) do reset the BatchNorm statistics in their interpolated ResNet50s based on our suggestion to do so<sup>3</sup>. The extra barrier reduction in our results can therefore be attributed to the fact that REPAIR also statistically corrects the outputs of each residual block.

## C Additional plots

<sup>3</sup>See <https://twitter.com/kellerjordan0/status/1570837651741364226> and Section A.3.3 of Ainsworth et al. (2022) <https://arxiv.org/abs/2209.04836v3>.

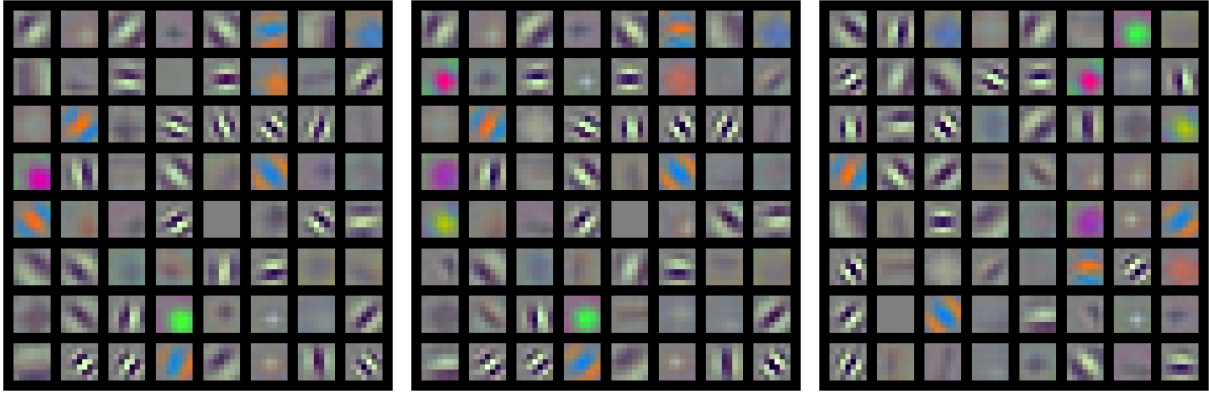


Figure 9: **Aligned convolutional filters for the first layer in ResNet50.** We train two ResNet50s on ImageNet independently, calling these models A and B. **Left:** The first-layer convolutional filters of model A. **Middle:** The filters of model B, having been permuted in order to maximize the total activation-wise correlation to the corresponding filters of model A. Some paired filters appear nearly identical, while for others there was no close match. **Right:** The filters of model B in their original positions.

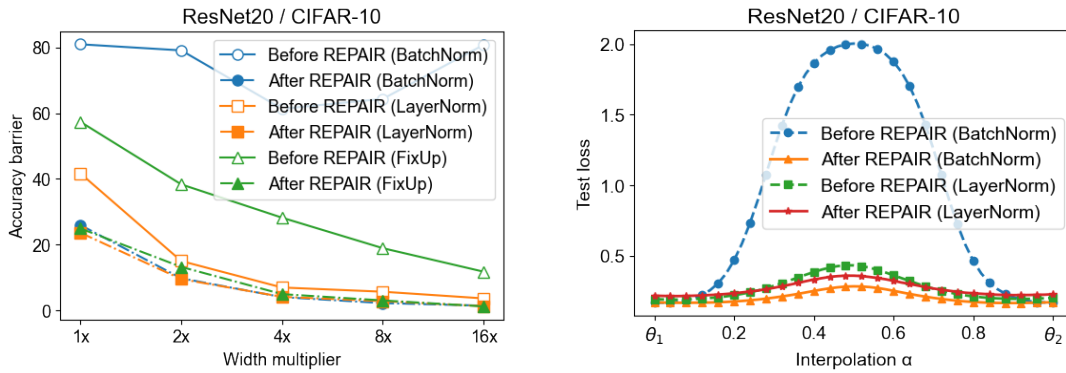


Figure 10: **Effect of normalization layer.** **Left:** We replicate Figure 4 (left) with barriers measured in terms of test accuracy. **Right:** We replicate Figure 4 (right) with barriers measured in terms of test loss.

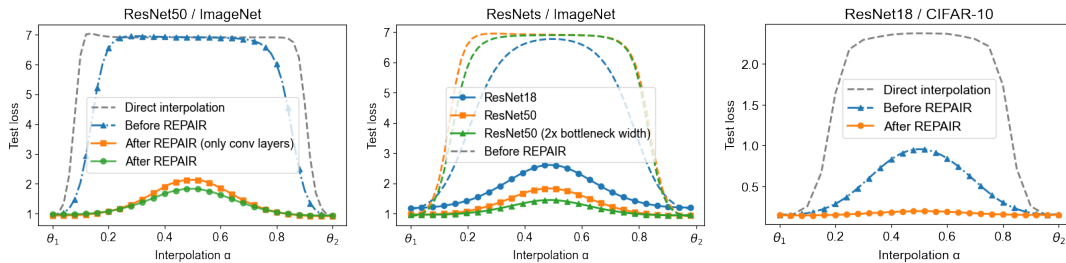


Figure 11: **Barrier curves in terms of loss.** We report the performance of interpolated ResNets in terms of test loss on ImageNet and CIFAR-10. The corresponding figures in terms of accuracy are Figure 5 and Figure 3 (middle).

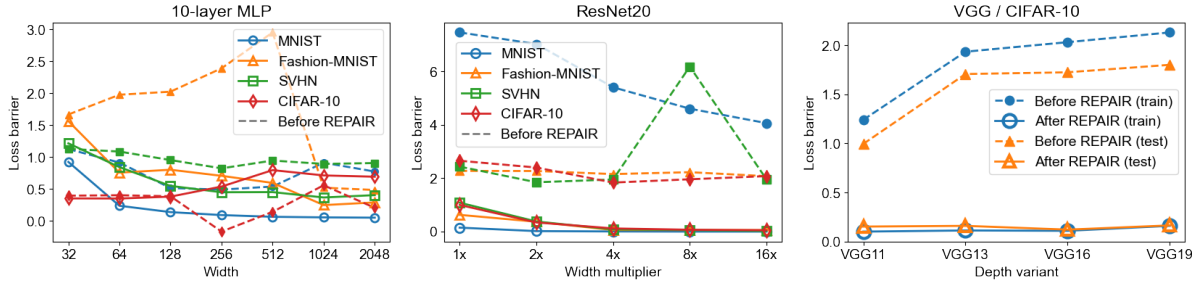


Figure 12: **Network width and depth.** We replicate Figure 6 with barriers measured in terms of test loss instead of test accuracy.

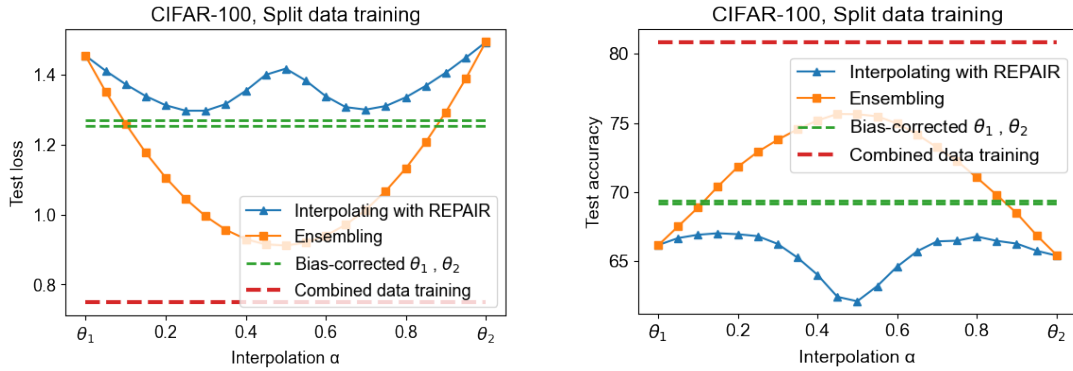


Figure 13: **CIFAR-100 split data experiment against a baseline.** Two networks are independently trained on disjoint, biased subsets of the CIFAR-100 training set. With respect to performance on the full CIFAR-100 test set, we report the performance of ensembling/mixing the logit outputs of the two models (orange), and the performance of interpolations in weight-space between two aligned models (blue), with REPAIR applied to every interpolated network. As baselines, we report the performance of a single model which was trained on the full CIFAR-100 training set (red), and the performance of the two endpoint networks, after a distribution-shift correction has been applied (green). We find that there exist REPAIRED interpolated checkpoints which outperform either endpoint network in terms of both test loss and accuracy, showing that constructive merging of models is possible. The distribution-shift correction (green line) is as follows. Consider an endpoint network A; it was trained with a training set that was biased 4:1 towards the first 50 classes, so that on the test set, network A over-predicts these first 50 and under-predicts the second 50 classes, leading to increased loss. Our baseline is then to scale down the first 50 logits of network A such that its predictions on the test set become balanced over the 100 classes. We find that this baseline, applied separately to either endpoint network (thus two green lines), outperforms the best gain that can be obtained from constructive merging of the two models via REPAIRED interpolation.

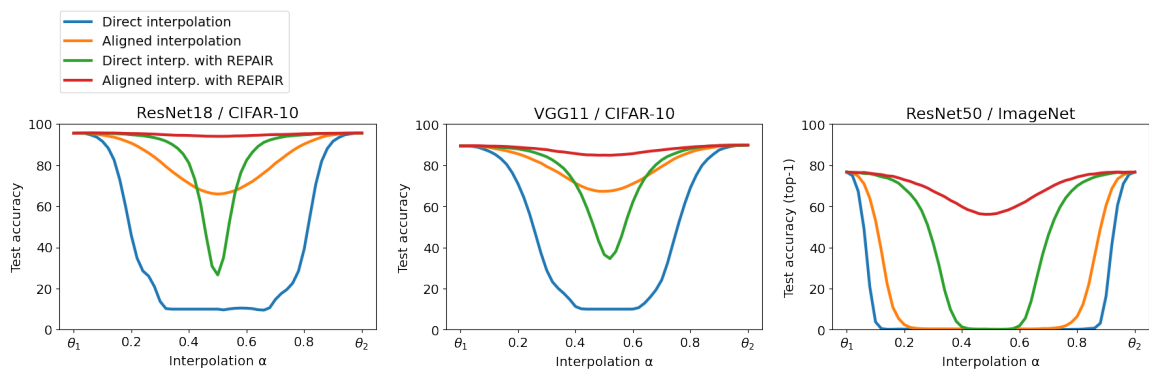


Figure 14: **REPAIR without alignment.** In the preceding experiments, we have always first aligned the neurons of the two endpoint networks before interpolating. In this figure we also report accuracy curves for interpolations between the original unaligned endpoint networks, both with and without REPAIR. We note that in the case of ResNet18, we apply REPAIR to convolutional outputs, which is exactly equivalent to resetting BatchNorm statistics. For VGG11, the architecture does not contain normalization layers, and REPAIR is applied to convolutional outputs. For ResNet50, we apply REPAIR to both convolutional outputs and residual block outputs, as described in Section 5.2. It appears that REPAIR is effective towards the endpoints, and neuron-alignment becomes essential near the midpoint. Both methods are necessary in order to have a high-performing midpoint.